



King Saud University

Saudi Journal of Biological Sciences

www.ksu.edu.sa
www.sciencedirect.com



ORIGINAL ARTICLE

Modeling studies on mono and binary component biosorption of phenol and cyanide from aqueous solution onto activated carbon derived from saw dust

Neetu Singh^{*}, Anupama Kumari, Chandrajit Balomajumder

Indian Institute of Technology, Department of Chemical Engineering, Roorkee, India

Received 18 August 2015; revised 27 October 2015; accepted 3 January 2016

KEYWORDS

Binary-component modeling;
 Biosorption;
 Cyanide;
 Kinetics;
 Phenol;
 Thermodynamics

Abstract Biosorption is an effective treatment method for the removal of phenol and cyanide from aqueous solution by saw dust activated carbon (SDAC). Batch experiments were achieved as a function of several experimental parameters, i.e. influence of biosorbent dose (5–60 g/L) contact time (2–40 h), pH (4–12), initial phenol concentration (100–1000 mg/L) and initial cyanide concentration (10–100 mg/L) and temperature (20–40 °C). The biosorption capacities of the biosorbent were detected as 178.85 mg/g for phenol with 300 mg/L of initial concentration and 0.82 mg/g for cyanide with 30 mg/L of initial concentration. The optimum pH is found to be 8 for phenol and 9 for cyanide biosorption. The mono component biosorption equilibrium data for both phenol and cyanide were well defined by Redlich–Peterson model and binary component adsorption equilibrium data well fitted by extended Freundlich model. The percentage removal of phenol and cyanide using SDAC was 66.67% and 73.33%, respectively. Equilibrium established within 30 h for phenol and 28 h for cyanide. Kinetic studies revealed that biosorption of phenol followed pseudo second order indicating adsorption through chemisorption and cyanide followed pseudo first order kinetic model indicating adsorption through physisorption. Thermodynamic studies parameters, i.e., enthalpy (ΔH_0), entropy (ΔS_0) and Gibb's free energy (ΔG_0) have also been considered for the system. Thermodynamic modeling studies revealed that the process of cyanide biosorption was endothermic and phenol biosorption was exothermic in nature.

© 2016 The Authors. Production and hosting by Elsevier B.V. on behalf of King Saud University. This is an open access article under the CC BY-NC-ND license (<http://creativecommons.org/licenses/by-nc-nd/4.0/>).

^{*} Corresponding author.

E-mail addresses: neeturbs@gmail.com (N. Singh), kumari.anupama06@gmail.com (A. Kumari), chandfch@iitr.ernet.in (C. Balomajumder).
 Peer review under responsibility of King Saud University.



Production and hosting by Elsevier

<http://dx.doi.org/10.1016/j.sjbs.2016.01.007>

1319–562X © 2016 The Authors. Production and hosting by Elsevier B.V. on behalf of King Saud University.

This is an open access article under the CC BY-NC-ND license (<http://creativecommons.org/licenses/by-nc-nd/4.0/>).

Please cite this article in press as: Singh, N. et al., Modeling studies on mono and binary component biosorption of phenol and cyanide from aqueous solution onto activated carbon derived from saw dust. Saudi Journal of Biological Sciences (2016), <http://dx.doi.org/10.1016/j.sjbs.2016.01.007>

Nomenclature

Q_t	uptake of phenol and cyanide at time t (mg/g)	$\eta_{RP,i}$	multicomponent Redlich–Peterson model constant (l/g)
C_t	liquid phase concentration of phenol and cyanide at time t (h)	$a_{RP,i}$	multicomponent Redlich–Peterson model constant (l/mg)
C_i	initial pollutant concentration (mg/L)	β_j	multicomponent Redlich–Peterson model constant
C_{eq}	concentration of adsorbate at equilibrium (mg/L)	x_i, y_i, z_i	constant in modified Redlich–Peterson model
V	volume of the solution (L)	K_1	pseudo-first order model constant
M	weight of the adsorbent (g)	K_2	pseudo-second order model constant
q_e	specific uptake of adsorbent at equilibrium (mg/g)	K_{id}	intra-particle diffusion model constant
Q_o	Langmuir model constant (mg/g)	ΔG^0	change in Gibb's free energy (kJ/mole)
b	Langmuir model constant	Δs^0	change in entropy (kJ/mol K)
$Q_{e,i}$	amount of i th component adsorbed per gram of adsorbent at equilibrium (mg/g)	Δh^0	change in enthalpy (kJ/mole)
$Q_{o,i}$	modified Langmuir model constant for i th component (mg/g)	B_F	Bias factor
$C_{e,i}$	concentration of i th component in the binary mixture at equilibrium (mg/L)	NSD	Normalized Standard Deviation
K_F	Freundlich model constant (mg/g)	RMSE	Root Mean Square Error
n	Freundlich model constant	ARE	Average Relative Error
$K_{F,i}$	extended Freundlich model constant (mg/g)	MPSD	Marquardt's percent standard deviation
K_{RP}	Redlich–Peterson model constant (l/g)	N	number of observations in the experimental isotherm
a_{RP}	Redlich–Peterson model constant (l/mg)	P	number of parameters in regression model
β	Redlich–Peterson model constant	$Q_{e,i}^{exp}$	experimental value of Q_e (mg/g)
		$Q_{e,i}^{cal}$	predicted value of Q_e (mg/g)

1. Introduction

Development of new and unconventional technologies as well as improvement of existing technologies have been done for the treatment of wastewater in accordance with the several standards related to the discharge of impurities into water and soils. The toxic pollutants like phenol and its derivatives (Pyro-catechol, Quinone), ammonia, rhodanate and cyanide are present in wastewater which is discharged from the petrochemical and coke industry and the wastewater produced in the process of coking and coal liquefaction. These pollutants are extremely dangerous for the natural environment and human health (Kowalska et al., 1998). A concentrated liquid effluent excluded from the production unit of coke industry, must be treated prior to discharge or recycled without any dangerous effect. Wastewater generated from coke oven by-product of an integrated iron and steel industry is described as the most polluted. Various chemicals like phenol, cyanide and ammonia are present in this wastewater. These untreated chemicals are more harmful for the water bodies in which they are discharged. The effects of these pollutants on the water bodies are: aquatic life toxicity, reduction in dissolve oxygen (DO), suspended solids silting, taste and odor, temperature rise, which affects the dissolved oxygen and aquatic life and oil slicks formation due to floating oil (Biswas, 2013). Due to increasing water and lack of public awareness, various new treatment methods are established for proper treatment of wastewater. Both phenol and cyanide are highly toxic and their toxicity depends upon their physicochemical properties. The interaction of phenol to human environment can harm the human skin, damage the liver, increase the irregularity of heartbeat and lastly death. At low concentrations, phenol compounds had a toxic effect on humans by ingestion, contact or

inhalation because the vapor of phenol can be easily absorbed through the skin and it also affects the metabolic activity of the living system (Chung et al., 2003). Most toxic forms of cyanide are inorganic cyanides which are extremely harmful when consumed and become more toxic when they are mixed with water. The water soluble constituents of cyanides are sodium, potassium and inorganic cyanides. Due to the solubility properties with water, these cyanides make solutions in the human stomach and quickly enter the blood. Some regulations have been applied to the discharge of effluents containing cyanide and phenol by several environmental agencies. The maximum allowable limit of cyanide and phenol in discharge effluents proposed by Unites States Environmental Protection Agency (USEPA) and the Minimum National Standard (MINAS) of the Central Pollution Control Board (CPCB) of India is 0.2 mg/L and 0.5 mg/L, respectively (Vedula et al., 2013).

Various methods are applied for phenol and cyanide degradation along with co-toxicants. These methods are precipitation, coagulation, ion exchange and ultra-filtration, but these methods are more expensive and insufficient because of the by products produced, as a result these methods are becoming more toxic in nature (Busca et al., 2008; Dash et al., 2009). The possible technologies applied for the wastewater treatment comprising phenol and thiocyanate are ozonation, chlorination, solvent extraction, adsorption, membrane process, biological and coagulation treatment. But due to the formation of secondary toxic materials such as cyanates, chlorinated phenols and hydrocarbons, these treatment methods are not favorable for the environment (Bandyopadhyay et al., 1998; Agrawal et al., 2013). Hence, the biosorption process is preferred mostly for the removal of cyanide and phenol. The biosorption treatment is easily operated and also this treatment process is not affected by the toxic effect of phenol and

cyanide and there is no need of hazardous chemicals in the process (Gupta et al., 2012).

Biosorption method for the wastewater treatment has been proved to be an economical process due to various advantages, i.e. low cost, profitable, easily available, easily operated and good efficiency. Biosorption process has been demonstrated to be one of the most effective technologies for the academic and industrial world for the complete removal of pollutants. Various experiments have been done for the biosorption process using different biosorbents. Some most useful biosorbents include bentonite, saw dust, peat, fly ash, prawn, waste, leaves, vegetable and fruit peels etc (ATSDR, 2006; ATSDR, 2008; Jadhav and Vanjara, 2004; Malik, 2004; Mandi et al., 2009; Prasad and Santhi, 2012; Santhi and Manonmani, 2012; Viraraghavan and Alfaro, 1998).

Activated carbons have been found to be distinctive and resourceful biosorbents due to their considerable surface area, micro porous structure and high biosorption capacity. But activated carbons have been avoided due to the high cost (Nwufu et al., 2014). Owing to this disadvantage, the preparation of activated carbons from various cheaper materials has become one of the best alternative methods for the treatment of wastewater through biosorption. Activated carbon (AC), resulting from wood, bagasse ash, coconut shells, and agriculture waste has been extensively used for the elimination of a number of pollutants from wastewater (Dwivedi et al., 2008). One of the cheap materials for biosorption is sawdust activated carbon due to its natural availability from various sawmills as solid waste at minimal cost. Sawdust is a secondary product produced from cutting, grinding, drilling, sanding and slicing of wood from saw or other instrument. In this study, saw dust, which has low commercial value, was used for the preparation of activated carbon and its capacity to the elimination of phenol and cyanide from aqueous solution was studied.

The main objective of this current study is to carry out the studies on the equilibrium isotherm, kinetics, and mechanism of phenol and cyanide biosorption onto sawdust activated carbon as biosorbent. This study provides insight into phenol and cyanide biosorption in terms of kinetic and equilibrium from aqueous solutions. It also offers significant information that could be used in the optimization and design of phenol and cyanide biosorption process. Consequently, work is aimed at estimating the diffusion and kinetics parameters for the biosorption of phenol and cyanide onto SDAC and to evaluate the feasibility of SDAC for the biosorption process. The effects of several parameters such as dose, time, pH, temperature, and initial concentration are considered and results acquired are discussed.

2. Materials and methods

2.1. Chemicals and solution preparation

All the analytical grade reagents were used in this study. Stock solutions of 1000 mg/L and 100 mg/L comprising only phenol or cyanide or mixture of these two components were prepared by dissolving proper amounts of phenol and cyanide in double distilled deionized water (Milli-Q Millipore 18.2 M/cm conductivity). To prepare the solutions of suitable concentration 100–1000 mg/L of phenol and 10–100 mg/L of cyanide, the stock solution was diluted with double distilled water. The

Regulation of pH was undertaken using 0.1 N HCl and 0.1 N NaOH.

2.2. Sawdust activated carbon preparation

Sawdust was taken from the local market Roorkee, for the preparation of biosorbent. The sawdust was washed with distilled water and the supernatant solution was separated to avoid color leaching and water soluble impurities. Several iterations of this procedure were done to get a clear supernatant solution. Finally, the washed biosorbent was dried at 60 °C in an oven for 12 h. The saw dust activated carbon was prepared using the chemical activation method. For this purpose the dried saw dust was kept with 2 N H₂SO₄ in a muffle furnace at temperature 200 °C for 12 h in the ratio of 1:3 by solid to liquid. The saw dust activated carbon (SDAC) was washed with millipore water to eliminate residual chemicals and then the sample was dried at 60 °C temperature for 24 h. After that the sample was additionally soaked into 1% NaHCO₃ solution and kept overnight for complete elimination of acid. The product obtained by this process was washed with double distilled deionized water until superficial liquid was acquired and dried at 60 °C for 12 h. Finally, the SDAC were stored in air tight poly bag for further use.

2.3. Batch experiments for biosorption

In this study biosorption has been done using synthetic/simulated wastewater prepared in a laboratory. Optimization of parameters of batch experiments was implemented in a 250 ml round bottom flask with working solution of 100 ml at 125 rpm in an incubator cum orbital shaker (Metrex, MO-250, India). To develop a binary component system, the ratio of 10:1 has been taken between phenol and cyanide concentration. This ratio is also observed in coke wastewaters. In continuation of the experiment, the incubator was shielded with black cardboard perfectly to stop photo oxidation of phenol and cyanide. The experiments were performed in triplicate and average results of triplicate were used. The initial concentration of adsorbate was set at 300 mg/L for phenol and 30 mg/L for cyanide. The pH and temperature were chosen from the range of pH 4–12 and temperature 20–40 °C optimally. The optimal dose of biosorbent was selected as 5–60 g/L on the basis of maximum percentage removal of phenol and cyanide. Sufficient time of 40 h for all the experiments was provided to attain the equilibrium. In the case of any change during the experiment, pH of the solution was examined after every 2 h and reset to previous value with the help of 1 N NaOH or HCl. Initial concentration of phenol and cyanide was altered from 100 to 1000 mg/L and 10–100 mg/L, respectively for the study of adsorption isotherms. After every 2 h till the equilibrium conditions reached, an assumed volume of the sample was taken for the study of biosorption kinetics. This sample was filtered by standard what man filter paper (Cat No. 1001 125) and then the filtrate was analyzed for phenol and cyanide by 4-Aminoantipyrine and colorimetric picric acid method, respectively (APHA, 2001).

The adsorbed amount of phenol and cyanide per unit mass of the biosorbent at equilibrium (Q_{eq}) and at time t (Q_t) was designed using the following equation:

$$Q_{eq} = (C_i - C_{eq})V/M \quad (1)$$

$$Q_t = (C_i - C_t)V/M \quad (2)$$

The percent removal of phenol and cyanide was calculated as follows:

$$\text{Percentage removal} = ((C_i - C_f)/C_i) * 100 \quad (3)$$

where

Q_{eq} is the amount of phenol and cyanide adsorbed on to the per unit mass of biosorbent at equilibrium (mg/g)

Q_t is the uptake of phenol and cyanide at time t (mg/g)

C_f is the final concentration of phenol and cyanide (mg/L)

C_t is the liquid phase concentration of phenol and cyanide at time t (h)

C_i is the initial concentration of phenol and cyanide (mg/L)

C_{eq} is the concentration of adsorbate at equilibrium (mg/L)

V is the volume of the solution (L),

M is the weight of the biosorbent (g).

Equilibrium isotherm and thermodynamic modeling studies were achieved by varying the initial concentration of phenol and cyanide solution 100–1000 mg/L and 10–100 mg/L, respectively, and the reaction temperature (20–40 °C). Kinetic studies were accomplished by changing the phenol and cyanide concentration and samples were collected at every 2 h time intervals till equilibrium was reached.

2.4. Adsorption isotherms

The process of biosorption is explained by the isotherms which are defined as the curve drawn for the functional relationship between the adsorbate and the biosorbent for a constant temperature adsorption process. Mechanism of adsorption is conducted by various controlled reactions or physical phenomena containing large change in reaction times from seconds to years (Al-Asheh et al., 2000).

The experimental data are fitted with the various single component isotherm models i.e. Langmuir, Freundlich, Redlich-Peterson Toth and Fritz-Schlunder. These models describe the distribution of ions of components between the solid phase and liquid phase. For the binary component isotherm study several multicomponent isotherm models also used in this study such as, modified Langmuir, non-modified Langmuir, extended Langmuir, extended Freundlich, modified Redlich-Peterson and non-modified Redlich-Peterson models (Agrawal et al., 2013; Kumar et al., 2011).

2.4.1. Mono component isotherm models

The Langmuir isotherm relates the quantitative description of the development of a biosorbent monolayer on the outer surface of the biosorbent and no further biosorption performed after it. This isotherm has described the biosorption process applied onto activated carbon in solid-liquid phase. In this isotherm, it is assumed that there is equal distribution of energies of biosorption on the surface and there is no movement of the adsorbate in the plane of the surface. The non-linear form of the Langmuir isotherm model is represented by the subsequent equation:

$$Q_e = (Q_0 b C_e)/(1 + b C_e) \quad (4)$$

where C_e the concentration at equilibrium condition in mg/L is, Q_0 is the amount of adsorbed ion in mg/g, and b is the adsorption equilibrium constant in L/mg.

A dimensionless constant i.e. separation factor for the Langmuir isotherm represents the affinity between the sorbet and sorbent and calculated from the relation given:

$$R_l = \frac{1}{(1 + b C_0)} \quad (5)$$

The specification of the Langmuir isotherm can be indicated by R_l for example $R_l = 0$ indicates irreversible, $0 < R_l < 1$ indicates favorable, $R_l = 1$ indicates linear and $R_l > 1$ indicates unfavorable isotherm (Carvalho et al., 2007).

Freundlich isotherm is not only concerned for the monolayer configuration, but also concerned with the non-ideal and reversible biosorption. Freundlich isotherm gives the relation for the solute concentration on to biosorbent surface and the solute concentration in the liquid through which it is contacted. Particularly this isotherm is the expression for the heterogeneous surface energies through which the term (Q_m) in the Langmuir isotherm varies as the function of the amount of adsorbed ion due to changes in the heat of biosorption (Carvalho et al., 2007). The mathematical expression for this isotherm, which specifies the empirical model for the biosorption are given:

$$Q_e = K_f C_e^{1/n} \quad (6)$$

where q_e is the adsorbed amount per biosorbent amount at equilibrium in mg/g, C_e is the concentration at the equilibrium mg/L and K_f and n are the parameters which depend upon the adsorbate and biosorbent. In Freundlich isotherm, $n = 1$ indicates linear biosorption, $n > 1$ indicates physical process and mostly found because of the distribution of surface site or any disturbance which is the basis of the decrease in the interaction between the biosorbent and adsorbate with the increase in density of surface (Huh et al., 2000), $n = 1-10$ indicates good biosorption (Korhonen, 2011), and $n < 1$ indicates the chemical process (Desta, 2013). The Freundlich isotherm fails at high pressure due to the saturation in the biosorption rate at saturation pressure.

The Redlich-Peterson isotherm includes the features of both Langmuir and Freundlich isotherm which combine three parameters into an equation. At high concentration, Redlich-Peterson isotherm resembles Freundlich isotherm and at low concentration, it follows the ideal Langmuir model. Mathematically, Redlich-Peterson isotherm can be represented as:

$$Q_e = \frac{K_{RP} \cdot C_{eq}}{1 + a_{RP} \cdot C_{eq}^\beta} \quad (7)$$

where K_{RP} and a_{RP} are Redlich-Peterson isotherm model constants and β is exponent of Redlich-Peterson isotherm, which lies between 0 and 1 (Carvalho et al., 2007). For $b = 1$, the model equation is converted to the Langmuir isotherm model equation.

2.4.2. Binary component isotherm models

In an aqueous solution, the existence of more than one component can cause interference and competition for adsorption sites. This establishes a more problematic mathematical formulation of equilibrium. Hence, the relationship between the adsorbed amount of one component and concentrations of

other components in the aqueous solution are explained by multi component isotherm models (Aksu and Akpinar, 2008; Aksu and Acikel, 2000; Aksu et al., 2002; Ho and McKay, 1998). Non-modified models utilize the parameters obtained from mono component models, however, modified models utilize the parameters of mono component models with correction factors.

Non-modified Langmuir model:

$$Q_{e,i} = (Q_{0,i} b_i C_{e,i}) / \left(1 + \sum_{j=1}^N b_j C_{e,j} \right) \quad (8)$$

Modified Langmuir model:

Behavior of binary component biosorption may not be defined by constants of single biosorption. Hence, modified isotherms are developed for the better accuracy which is related to parameters of mono component isotherm and correction factors. An interaction term which is representative of all species and depends upon the concentration of the other components has been included in the modified Langmuir model. This term can be calculated from the experimental data on binary component system.

The modified Langmuir model:

$$Q_{e,i} = (Q_{0,i} b_i C_{e,i} / n_i) / \left(1 + \sum_{j=1}^N b_j (C_{e,j} / n_j) \right) \quad (9)$$

Extended Freundlich model:

For the binary solutions, the empirical extended Freundlich model has been developed which is given by the following equations for each component of binary solutions:

$$Q_{e,i} = (K_{F,i} C_{e,i}^{1/n_i + x_i}) / (C_{e,i}^{x_i} + y_1 C_{e,j}^{x_j}) \quad (10)$$

$$Q_{e,j} = (K_{F,j} C_{e,j}^{1/n_j + x_j}) / (C_{e,j}^{x_j} + y_2 C_{e,i}^{x_i}) \quad (11)$$

Non-modified Redlich Peterson model:

For the multi component system, a non-modified Redlich–Peterson model has been established which is given by the following equation:

$$Q_{e,i} = K_{RP,i} \cdot C_{eq,i} / 1 + \sum_{j=1}^N a_{RP,j} (C_{eq,j})^{\beta_j} \quad (12)$$

Modified Redlich–Peterson model:

For the binary component system, a Redlich Peterson model has been developed with some modification implemented in it and known as the modified Redlich Peterson model which is given by the following equation:

$$Q_{e,i} = K_{RP,i} \cdot \left(\frac{C_{eq,i}}{\eta_{RP,i}} \right) / 1 + \sum_{j=1}^N a_{RP,j} \left(\frac{C_{eq,j}}{\eta_{RP,j}} \right)^{\beta_j} \quad (13)$$

2.5. Validation of the isotherm model

To validate the model for the mono component and binary component equilibrium adsorption data, the Marquardt's percent standard deviation (MPSD) was utilized as the following equation:

$$\text{MPSD} = 100 \sqrt{\frac{1}{n-p} \sum_{i=1}^p \left(\frac{Q_{e,i}^{\text{exp}} - Q_{e,i}^{\text{cal}}}{Q_{e,i}^{\text{exp}}} \right)^2} \quad (14)$$

Some statistical indices for the mono component system are introduced to see the validation of the model to the experimental data and to predict the accuracy of the models developed in this study (Panagou and Kodogiannis, 2009). The minimum value of statistical indices shows the more accurate estimation.

The following statistical measure between the experimental and calculated values used as following:

$$B_{\text{Fac}} = 10 \left(\sum \log_{10} (Q_{e,\text{cal}} / Q_{e,\text{exp}}) / N \right) \quad (15)$$

$$\text{NSD} = \sqrt{\frac{\sum (1 - Q_{e,\text{cal}} / Q_{e,\text{exp}})^2}{N}} \times 100 \quad (16)$$

$$\text{RMSE} = \sqrt{\frac{\sum (Q_{e,\text{exp}} - Q_{e,\text{cal}})^2}{N}} \quad (17)$$

2.6. Kinetic study

Kinetic studies for biosorption give the relation between the rate of the adsorbate uptake on biosorbent and which also controls the equilibrium time. These parameters calculated from the kinetic studies are beneficial in the determination of the rate of adsorption and provides useful information for the process modeling and designing. Three kinetic models are used for analyzing the kinetic parameters (Hameed et al., 2008).

Pseudo first order and pseudo second order models have been used for determination of the nature of biosorption: physical and chemical respectively, whereas the intraparticle model has been used for the study of mass transfer effects. Several types of kinetic models described by Eqs. (18)–(20) are used in this study (Ho and McKay, 1998; Hoa and Ofomaja, 2006; Lagergren, 1898; Subramanyam and Das, 2009; Tsibranska and Hristova, 2011).

Pseudo first order

To predict the sorption kinetics, the pseudo first order model has been used, which is expressed as follows:

$$Q_t = Q_{eq} (1 - \exp(-K_1 t)) \quad (18)$$

Pseudo second order

Based on the equilibrium adsorption, the pseudo second order model is indicated by the following equation:

$$Q_t = k_2 Q_{eq}^2 t / (1 + Q_{eq} K_2 t) \quad (19)$$

Intraparticle

$$Q_t = K_{id} \times t^{0.5} \quad (20)$$

where k_1 and k_2 are the rate constants of pseudo first order and pseudo second order models (g/mg h) respectively. Q_{eq} and Q_t are the amounts of phenol and cyanide adsorbed per unit mass of biosorbent at equilibrium and at time t , respectively, and can be calculated by Eqs. (1) and (2).

The values of the rate constants of pseudo-first order model, pseudo-second order model and intraparticle diffusion model have been predicted by non-linear regression study of experimental data using Eqs. (18)–(20) for both phenol and cyanide onto SDAC. The better fit of the experimental data to the suggested kinetic models is usually shown by lower ARE values (Behnamfard and Mohammad, 2009).

$$\text{ARE} = 100/n \sqrt{\sum_{i=1}^p \left(\frac{Q_{e,i}^{\text{exp}} - Q_{e,i}^{\text{cal}}}{Q_{e,i}^{\text{exp}}} \right)^2} \quad (21)$$

where $Q_{e,i}^{\text{exp}}$ is the experimental Q_{eq} and $Q_{e,i}^{\text{cal}}$ is the equivalent calculated Q_{eq} according to kinetic model, n is the number of observations and p is the number of parameters.

2.7. Thermodynamic study

The thermodynamic modeling study provides significant information about the change in entropy and enthalpy during the process. The thermodynamic parameters provided information about the spontaneous nature of phenol and cyanide adsorption. Van't Hoff equation was used to evaluate the thermodynamic parameters such as change in Gibbs free energy (ΔG^0), change in enthalpy (Δh^0) and change in entropy (Δs^0) during the process (Khalid et al., 2005; Srihari and Das, 2008).

$$\ln k = \frac{\Delta s}{R} - \frac{\Delta h}{RT} \quad (22)$$

$$\Delta G^0 = -RT \ln k \quad (23)$$

where R is gas constant = 8.314×10^{-3} kJ/mole/K, ΔG^0 is kJ/mole, T = temperature in °K, Δs^0 is kJ/mol K, Δh^0 is the kJ/mole, and k is the equilibrium constant (amount on biosorbent/amount in solution).

3. Results and discussion

3.1. Characterization of biosorbent

The moisture content, ash content and fixed carbon for SDAC were found to be 6.98%, 4.07% and 21.87%, respectively. The bulk density of biosorbent was determined using MAC bulk density meter, which was found to be 435 kg/m³. The BET surface area was found to be 998.08 m²/g.

The FTIR spectroscopy is a significant systematic technique, which identifies the vibration features of functional groups that are available on biosorbent surfaces (Fig. 1). The

functional groups responsible for phenol and cyanide biosorption onto SDAC are definite by FTIR spectra. Peak around the section 2918.94 cm⁻¹ and 3381.45 cm⁻¹ indicates -CH and -OH functional group. A peak observed around 3635.06 cm⁻¹ indicates vibration of O-H group (free non-hydrogen bonded). The absorption peaks around 1022.03 established the occurrence of carboxyl groups in the CH₂-OH polysaccharide structure (Gok et al., 2011). Peaks at 1369.77 cm⁻¹ were the stretching of O-H functional groups. The strong band within 1075–1000 cm⁻¹ is owing to CH₂-OH group, which is the representative peak for polysaccharides (Srividya and Mohanty, 2009). The peak around 1610.28 cm⁻¹ relates to owing to the occurrence of carboxyl and carbonate structures, conjugated hydrocarbon groups, carboxylic groups and aromatic hydrocarbons, representing biosorption of phenol, whereas peak at 1369.77 cm⁻¹ relates to inorganic nitrates indicating a possible biosorption site for cyanide. The change was the disappearance of peaks at 3381.45 cm⁻¹, 1711.05 cm⁻¹, 1608.20 cm⁻¹, 1217.78 cm⁻¹ and 1049.11 cm⁻¹ indicating a decrease of -OH, stretch of COOH, C-OH and CH₂-OH group on the surface of biosorbent. It is clear from the FTIR analysis that the possible mechanism of biosorption of phenol and cyanide on SDAC biomass may be owing to the appearance and disappearance of functional groups and chemical reactions with sites of biosorbent surface and also due to physical adsorption.

Scanning electron microscopy (SEM) is extensively used to study the surface morphology and characteristics of the biosorbent. In this present study, the surface morphologies of SDAC before and after adsorbing phenol and cyanide were associated by SEM analysis. The smooth morphology and porous structure of SDAC shown in Fig. 2(a) and Fig. 2(b) makes it suitable biosorbent as it increases the biosorption capacity. The SEM micrographs Fig. 2(a) indicates the occurrence of numerous pores on the biosorbent surface, and a uneven structure onto surface with a huge surface area. From Fig. 2(b), it could evaluate that small particle adheres to the SDAC surface. This may be due to the occurrence of phenol and cyanide onto SDAC surface. This is assumed to be effective biosorption of phenol and cyanide onto SDAC surface.

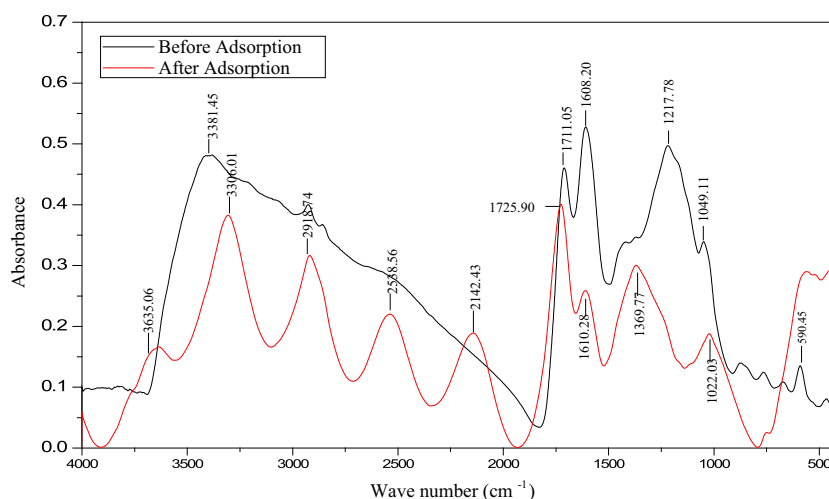


Figure 1 FTIR spectrum of biosorbent before and after biosorption.

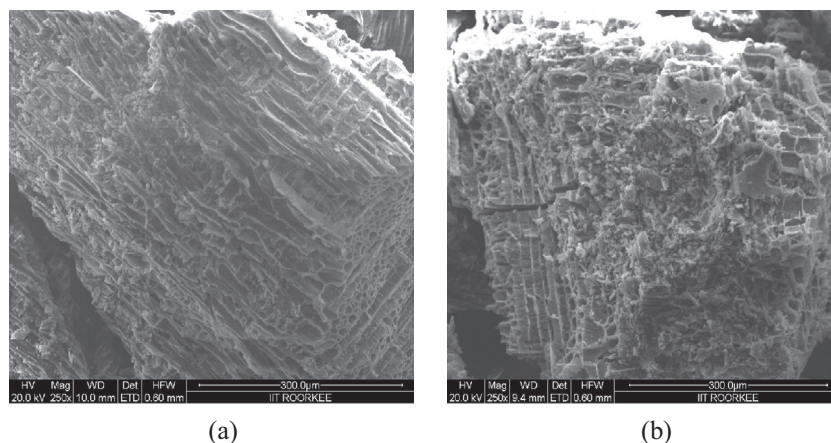


Figure 2 (a) SEM image of SDAC before biosorption and (b) SEM image of SDAC after biosorption.

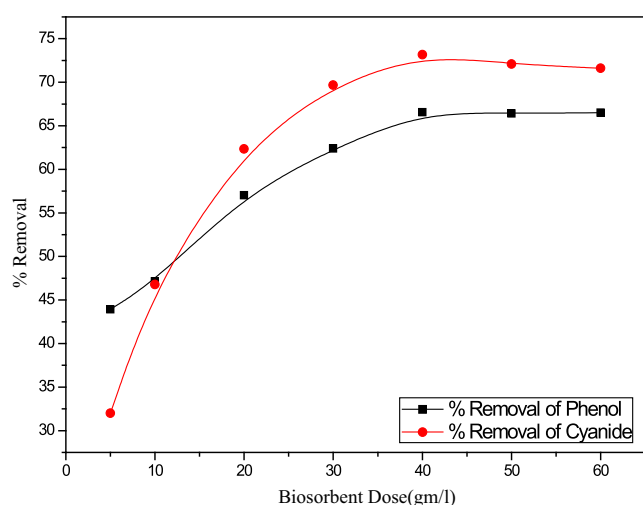


Figure 3 Influence of biosorbent dose on percentage removal.

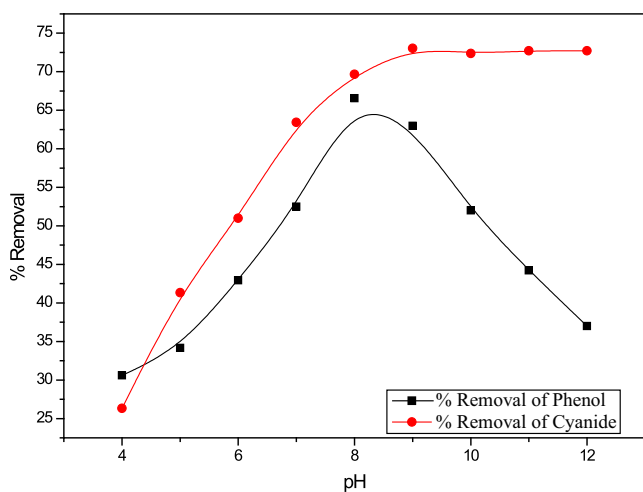


Figure 4 Influence of pH on percentage removal.

3.2. Influences of process parameters

3.2.1. Influence of biosorbent dose

Fig. 3 shows the effect on the percentage removal of phenol and cyanide with respect to different biosorbent dose. The percentage removal of phenol and cyanide is increasing with the increasing biosorbent dose up to 40 g/L and after that the percentage removal becomes constant with the increasing dose. This may be owing to accumulation of biosorbent particle resulting in decrease in surface area existing for biosorption (Kilic et al., 2011). Therefore, the selected optimum biosorbent dose of phenol and cyanide is 40 g/L with percentage removal of 66.55% for phenol and 73.16% for cyanide for the additional studies of biosorption.

3.2.2. Influence of pH

pH is a very essential parameter that influence biosorption procedure. **Fig. 4** indicates the effect on the percentage removal of phenol and cyanide with respect to varying pH (4–12). **Fig. 4** indicates the percentage removal of cyanide positively associates with pH of up to 9 and then remains almost constant (Saxena et al., 2001; Moussavi and Khosravi, 2010). So, pH 9 was measured as the optimum pH for biosorption by SDAC and the percentage removal of cyanide was 73.03%. Similar values of pH for biosorption of cyanide are stated in the works by Dash et al. (2009). On the other hand, the percentage removal of phenol is increasing with the increasing pH up to 8 after which the percentage removal of phenol is decreases with the increasing pH. The removal of phenol was found to decrease at low and high values of pH. At below pH 8 values, the phenol uptake is less owing to the existence of H^+ ions overwhelming the phenol ionization and hereafter its uptake on polar biosorbent is decreased. Though at pH more than its pK_a (9.96) a decrease in removal percentage is indicating biosorption of phenol mostly in its undissociated form. So, pH 8 was measured as the optimum pH for biosorption by SDAC and the percentage removal of phenol was 66.55%. Therefore, the selected optimum pH for phenol and cyanide biosorption is 8 and 9, respectively for further studies.

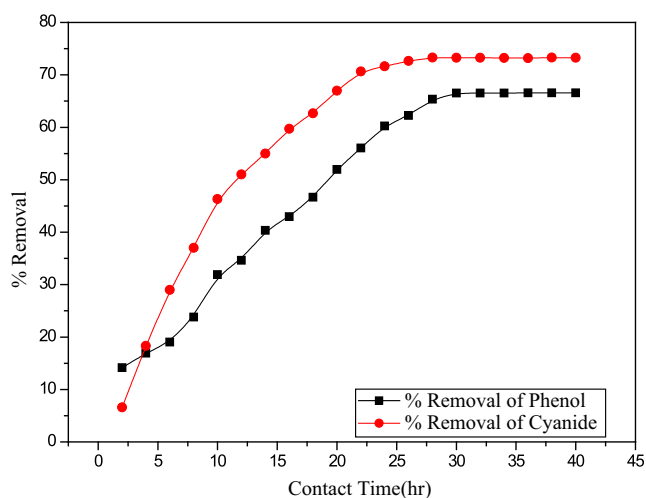


Figure 5 Influence of contact time on percentage removal.

3.2.3. Influence of contact time

Fig. 5 shows the effect on the percentage removal of phenol and cyanide at varying contact times. The percentage removal of cyanide was increasing with the increasing contact time till 28 h and after that the percentage removal of cyanide becomes constant with the increasing contact time. On the other hand, the percentage removal of phenol was increasing with the increasing contact time till 30 h, after which the phenol percentage removal continues leading to saturation with the increasing contact time. Maximum removal of phenol and cyanide was found at the initial stage of the experiment. The greater biosorption rate at the initial stage of the experiment can be recognized due to more vacant site available on the biosorbent surface at the initial stage (Ekpote et al., 2010; Uddin et al., 2007). Therefore, the selected optimum contact time for phenol and cyanide biosorption is 30 h and 28 h, respectively with percentage removal 66.55% for phenol and 73.3% for cyanide.

3.2.4. Influence of temperature

Fig. 6 shows the influence of the temperature (20, 25, 30, 35, and 40, °C) on the removal of phenol and cyanide. The amount of phenol eliminated from aqueous solution was slightly reduced by increasing temperature from 20 to 40 °C, which could be owing to the increased affinity of phenol desorption at increased temperature caused due to weakening of adsorptive forces between adsorbate and active sites of biosorbent and also between the nearby molecules of adsorbate (Saltali et al., 2007). The biosorption of cyanide was slightly greater than before with increased temperature from 20 to 40 °C. Though, the initial increase in biosorption with increase in temperature is possibly due to increase in active sites for biosorption. Similarly increase in temperature leads to reduction in viscosity of the solution and therefore, increase in the rate of the diffusion of adsorbate inside the pores (Sulaymon et al., 2013). The influence of temperature on removal of phenol and cyanide was not high. Therefore, the optimum temperature for the biosorption of phenol and cyanide was recognized as 30 °C. The maximum removal efficiency of phenol and cyanide was found to be 66.91% and 73.33%, respectively at 30 °C.

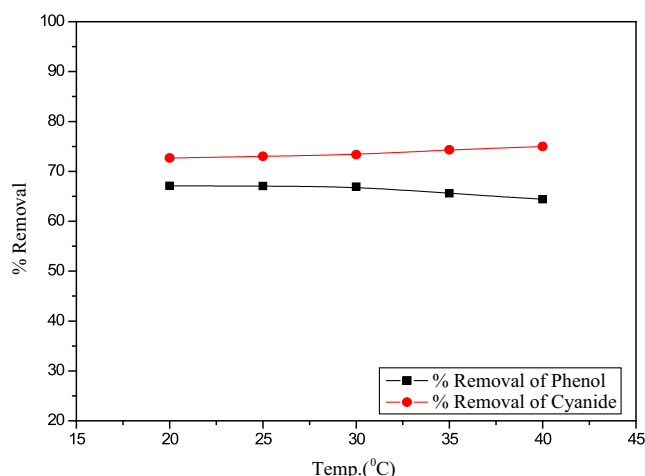


Figure 6 Influence of temperature on percentage removal.

3.2.5. Influence of initial concentration

Fig. 7(a) and (b) demonstrates the effect of percentage removal of phenol and cyanide at varying initial concentrations. The percentage removal of phenol and cyanide is decreasing with the increasing initial concentration. The more biosorption at the initial stage may be owing to more vacant sites available on the biosorbent surface at the initial stage. As the initial concentration of phenol and cyanide is increased there was a reduction in percentage removal. This can be recognized to the growth of phenol and cyanide particles on the biosorbent surface (Ekpote et al., 2010). The percentage removal of phenol decreases from 92.85% to 36.29% with the increasing initial concentration of phenol from 100 mg/L to 1000 mg/L and the percentage removal of cyanide decreases from 94.02% to 37.87% with the increasing initial concentration of cyanide from 10 mg/L to 100 mg/L.

3.3. Isotherm modeling

3.3.1. Mono component isotherm models

In batch biosorption studies, data demonstrate that SDAC has significant potential for the elimination of phenol and cyanide from aqueous solution. The equilibrium analysis for biosorption of phenol and cyanide on SDAC was analyzed by mono component adsorption isotherm models. The Redlich–Peterson adsorption isotherm model close-fitted with calculated phenol and cyanide concentration ranges at 30 °C. It was established that the values of MPSD attained from the Redlich–Peterson model are lower than those from Freundlich isotherm for phenol and Langmuir model for cyanide as given in Table 1. The value of dimensionless parameter R_f is established in the range of 0.176 to 0.021 for phenol and 0.0238 to 0.0303 for cyanide ($0 < R_f < 1$), which approves the favorable biosorption process. Table 1(a) indicates the value of statistical indices for phenol and cyanide biosorption. The value of model parameters and MPSD of the three isotherm models are given in Table 1(b). Fig. 8(a) and (b) shows the comparison between the three different isotherm models applied for phenol and cyanide removal. The order of the best fitted isotherm models for phenol are determined according to the lowest MPSD value, i.e. Redlich–Peterson > Freundlich > Langmuir. Whereas, the best fitted isotherm models for cyanide

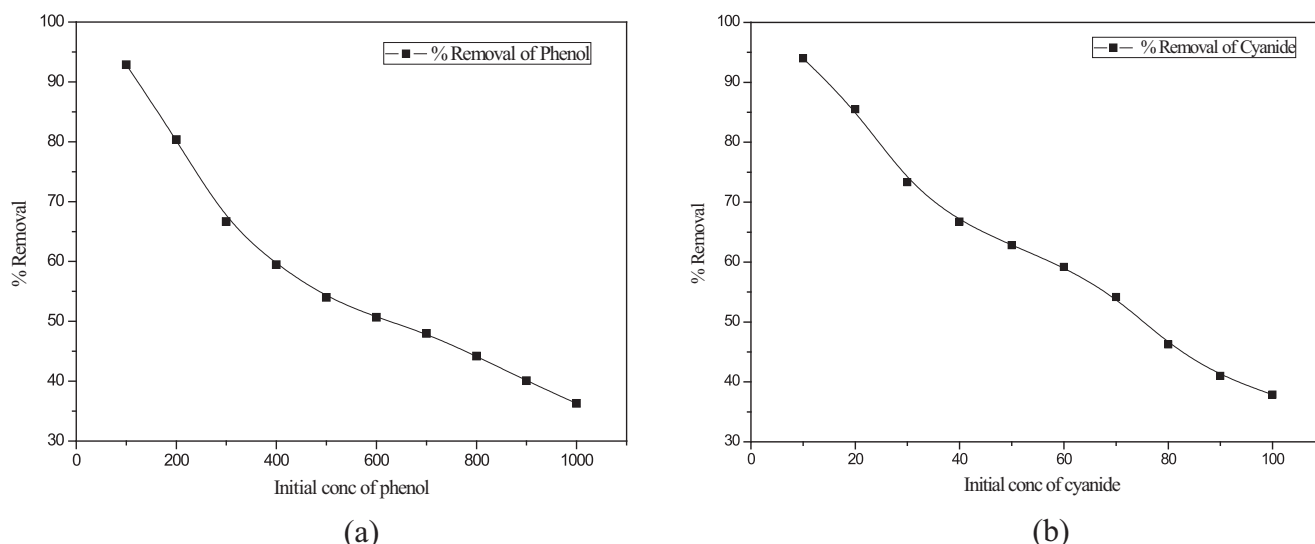


Figure 7 (a) Influence of initial phenol conc. on percentage removal and (b) influence of initial cyanide conc. on percentage removal.

Table 1(a) Statistical indices values of phenol and cyanide onto SDAC.

S. no	Models	Phenol			Cyanide		
		Bf	NSD	RMSE	Bf	NSD	RMSE
1	Langmuir model	0.98	12.27	0.50	0.99	6.31	0.02
2	Freundlich model	0.99	6.23	0.34	0.97	13.83	0.10
3	Redlich–Peterson model	1.00	4.10	0.21	1.00	4.75	0.03

Table 1(b) Models parameters of mono component adsorption equilibrium isotherm for SDAC.

Adsorbate	Langmuir model			Freundlich model			Redlich–Peterson model			
	Q_o	b	MPSD	K_f	$1/n$	MPSD	K_{RP}	a_{RP}	β	MPSD
Phenol	6.35	0.047	13.72	1.19	0.28	6.97	0.87	0.46	0.79	4.59
Cyanide	0.99	0.32	7.05	0.27	0.36	15.47	0.40	0.57	0.90	5.31

are: Redlich–Peterson > Langmuir > Freundlich. The maximum biosorption capacity acquired from the Langmuir isotherm model was 6.35 mg/g for phenol and 0.99 mg/g for cyanide. It can be observed from the figure that phenol has the maximum adsorption ability than cyanide onto SDAC.

3.3.2. Binary component isotherm models

Different binary component isotherm models were applied to the experimental biosorption data of phenol and cyanide on to saw dust activated carbon (Fig. 9a and b). Those isotherm models are non-modified Langmuir model, modified Langmuir model, extended Langmuir model, extended Freundlich model, non-modified Redlich–Peterson model and modified Redlich–Peterson model (Reynel-Avila et al., 2011). The calculated parameters of the binary component isotherm model are listed in Table 2. The multi component isotherm models represent the experimental binary adsorption data with different values of the degree of fit. On the basis of a graph drawn between experimental data and isotherm model and low MPSD value,

it has been observed that the best fit model has extended Freundlich model for both phenol and cyanide. The remaining models give the poor fit to the experimental data with a high value of MPSD for both phenol and cyanide. For SDAC biosorption of phenol followed the trend of better fit models as: extended Langmuir < modified Langmuir < non-modified Langmuir < modified Redlich Peterson < non-modified Redlich Peterson < extended Freundlich whereas biosorption of cyanide followed the trend: non-modified Redlich Peterson < extended Langmuir < non-modified Langmuir < modified Langmuir < modified Redlich Peterson < extended Freundlich. The maximum phenol and cyanide biosorption capacities have been found to be 178.85 mg/g of phenol with an initial concentration of 300 mg/L and 0.8211 mg/g for cyanide with an initial concentration of 30 mg/L.

The ratio of capacities of biosorption process ($Q_{q,i}$) is defined by the given formula:

$$Q_{q,i} = Q_{i,multi} / Q_{i,single}$$

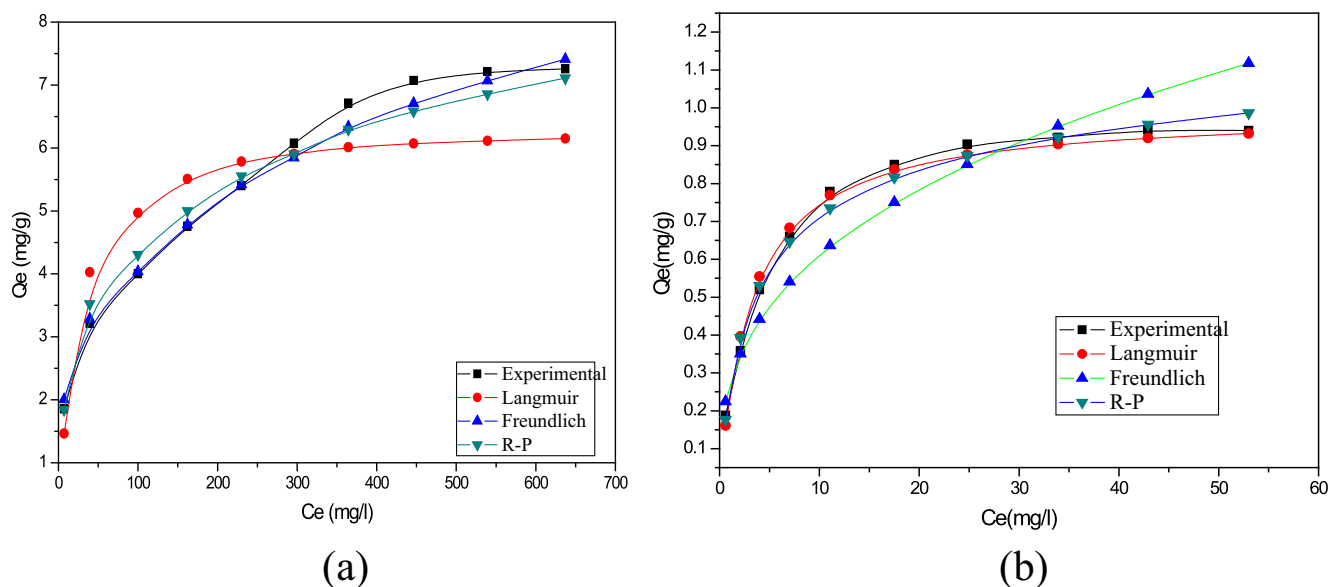


Figure 8 (a) Comparison of different mono component isotherm models for biosorption of phenol onto SDAC and (b) comparison of different mono component isotherm models for biosorption of cyanide onto SDAC.

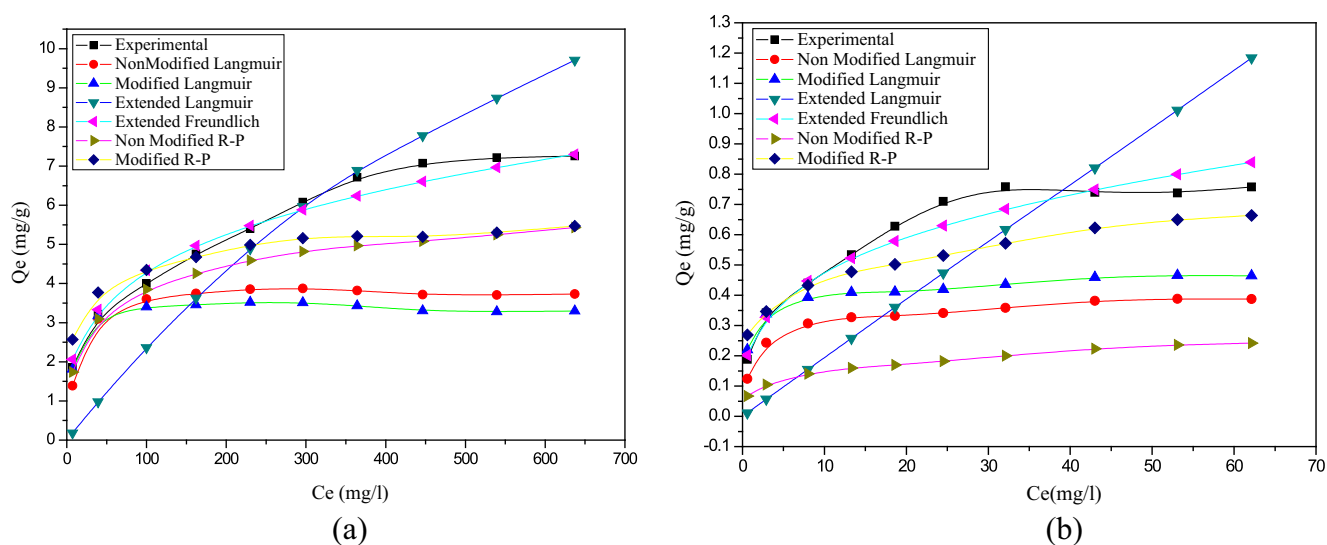


Figure 9 (a) Comparison of different binary component isotherm models for biosorption of phenol onto SDAC and (b) comparison of different binary component isotherm models for biosorption of cyanide onto SDAC.

where $Q_{i,multi}$ is the binary component adsorption capacity for component i in the binary solution and $Q_{i,single}$ is the mono component adsorption capacity of the same pollutant at the similar operating conditions of the binary solution. Parameter $Q_{q,i}$ permits to relate the binary component biosorbent performance to the results acquired in mono component systems using the same operating environments.

Literature designates that: 1: if $Q_{q,i} < 1$, the biosorption of component i is decreased by the presence of other components in the binary component aqueous solution (i.e., antagonistic adsorption). 2: if $Q_{q,i} > 1$, the presence of other components in binary component systems increases the adsorption of component i (i.e., synergistic adsorption), 3: if $Q_{q,i} = 1$, there is no effect on the binary component biosorption of component i (Reynel-Avila et al., 2011).

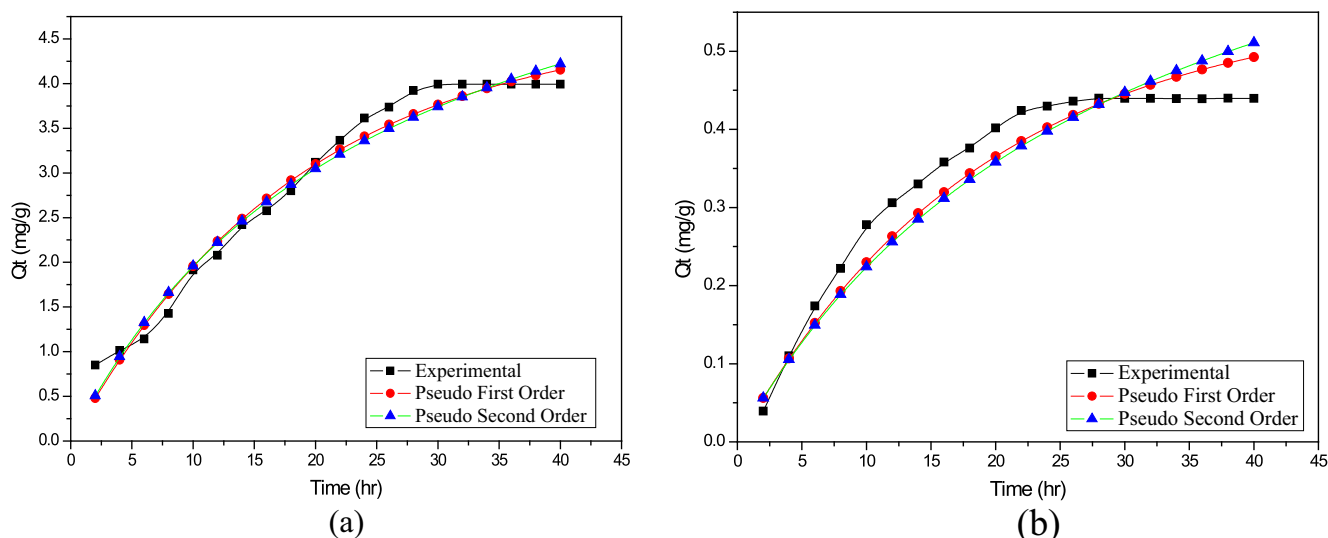
In the current study, for SDAC the ratio of $Q_{i,multi}/Q_{i,single}$ for phenol and cyanide was calculated as 28.17 and 0.83 hence substantiating the fact that phenol shows synergistic effects and cyanide indicates antagonistic biosorption effect.

3.4. Kinetic modeling

Various kinetic models have been introduced to define the mechanism of adsorption on the biosorbent surface. The biosorption of phenol and cyanide on to SDAC has been occurred due to physisorption or chemisorption process. The nature of process of biosorption can be determined by pseudo first order and pseudo second order kinetic models and can be analyzed by Fig. 10(a) and (b). Kinetic model parameters are

Table 2 Binary component model parameters list for SDAC.

Multicomponent isotherm model	Saw dust activated carbon (SDAC)		
	Parameters	Phenol	Cyanide
Non-modified Langmuir model	MPSD	38.99	48.83
Modified Langmuir model	$\eta_{i,j}$	0.5749	0.42
	MPSD	43.53	35.23
Extended Langmuir	$Q_{o,i}$	178.85	0.82
	b_i	0.0001	0.01
	MPSD	46.08	77.12
Extended Freundlich	x_i	0.0004	0.05
	y_i	0.00	0.12
	z_i	4.12	0.06
	MPSD	6.55	8.30
	MPSD	21.45	78.25
Non-modified Redlich–Peterson Model	MPSD	21.45	78.25
Modified Redlich–Peterson Model	$\eta_{i,j}$	0.16	0.06
	MPSD	24.15	22.80

**Figure 10** (a) Comparison experimental and calculated values of Q_t by pseudo-first and second order kinetic model for phenol adsorption onto SDAC and (b) comparison experimental and calculated values of Q_t by pseudo-first and second order kinetic model for cyanide adsorption onto SDAC.

presented in Table 3 for SDAC. Pseudo second order model is a better fit for phenol which indicated by lower ARE value, but ARE value of the pseudo second order model is slightly lower than that of the pseudo first order model so, the pseudo second order model is the best fit for phenol. In case cyanide pseudo first order indicates a good fit with a lower ARE value therefore, the kinetic experimental data are well fitted with pseudo first order model. Thus, the cyanide is adsorbed through physisorption and phenol is adsorbed through chemisorption as well as through physisorption (Tsibranska and Hristova, 2011). A graph between Q_t vs $t^{0.5}$ for phenol and cyanide shown is in Fig. 11(a) and (b), respectively. The plots consist of two step effect of the biosorption process. The initial portion of the plot indicates the external resistance to mass transfer adjacent the particle, while the next linear part dominated the regular biosorption phase through intra-particle diffusion (Srihari and Das, 2008). The first stage may also be recognized to the

Table 3 Kinetic models parameter list for SDAC.

Model	Parameters	Saw dust activated carbon	
		Phenol	Cyanide
Pseudo first order	Q_{tcal}	4.70	0.56
	K_{t1}	0.05	0.05
	ARE	2.60	2.99
Pseudo second order	Q_{tcal}	6.87	0.89
	K_{t2}	0.01	0.04
	ARE	2.52	3.29
Intraparticle	K_{id1}	0.61	0.06
	R_1^2	0.97	0.98
	K_{id2}	0.67	0.08
	R_2^2	0.42	0.05

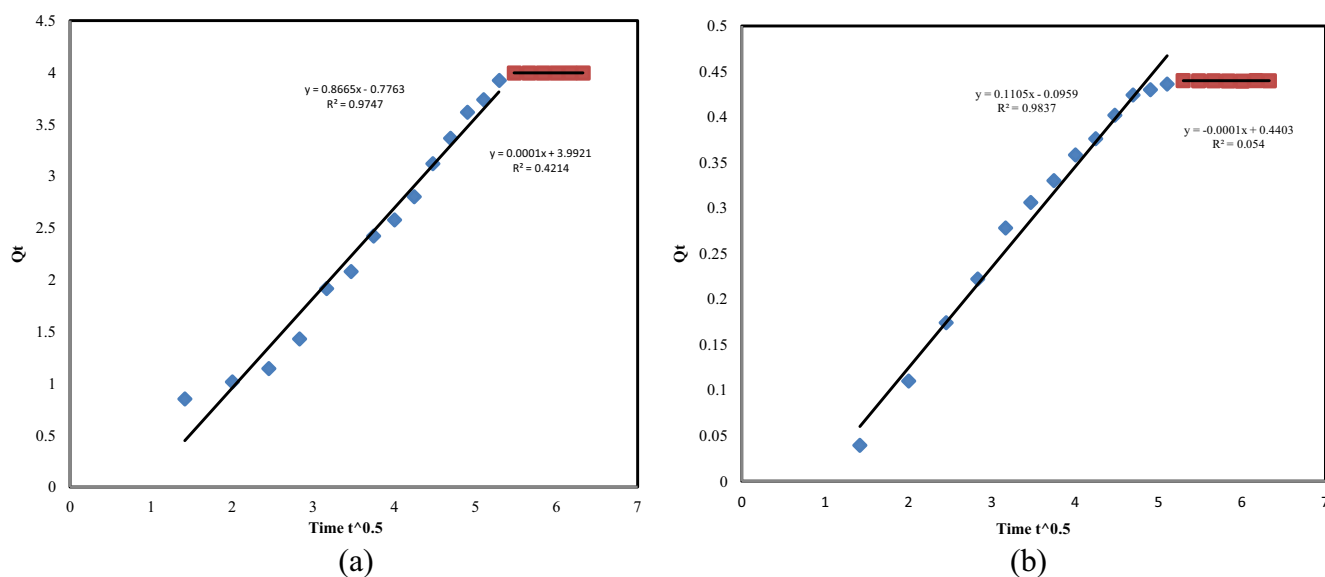


Figure 11 (a) Intraparticle diffusion model for phenol biosorption onto SDAC and (b) intraparticle diffusion model for cyanide biosorption onto SDAC.

Table 4 Thermodynamic model parameter list for SDAC.

Adsorbate	Temp. °C	Saw dust activated carbon			
		ΔG_0 (kJ mol ⁻¹)	Δh_0 (kJ mol ⁻¹)	Δs_0 (kJ mol ⁻¹ K ⁻¹)	R^2
Phenol	20	-17.37	-4.61	-0.01	0.82
	25	-17.62			
	30	-17.74			
	35	-16.53			
	40	-15.44			
Cyanide	20	-87.06	0.10	0.0002	0.94
	25	-88.85			
	30	-90.67			
	35	-93.17			
	40	-95.38			

boundary layer diffusion influence, whereas the second stage could be owing to intra-particle diffusion influences. The experimental data are better fit in the first region. Yet better fit of data in first region ($R_1^2 > R_2^2$) from Table 3 shows the control of surface diffusion in case of both phenol and cyanide biosorption (Allen et al., 1989). For intraparticle diffusion model as a rate controlling step, the plot should be passing through the origin (Mohanty et al., 2005).

3.5. Thermodynamic modeling

The values of Thermodynamic parameters as enthalpy (Δh_0), entropy (Δs_0) and Gibb's free energy (ΔG_0) are summarized in Table 4. For determining enthalpy (Δh_0) and entropy (Δs_0) a plot between $\log k$ vs $1/T$ was plotted according to Eq. (22). The enthalpy (Δh_0) change was positive (endothermic) for cyanide due to increase in biosorption with continual increase in temperature. The value of Δh_0 found negative shows the exothermic biosorption of phenol on SDAC

(Srihari and Das, 2008). Further, negative ΔG_0 values indicate a spontaneous process for both phenol and cyanide. The positive value of Δs_0 indicates the increased uncertainty at the solid-solution edge throughout the fixation of the cyanide on the active binding sites of the biosorbent. Then the biosorption process is endothermic for cyanide and exothermic for phenol. For SDAC the values of $\Delta h_0 = -4.61$ kJ/mol and $\Delta s_0 = -0.01$ J/mol were calculated for phenol and $\Delta h_0 = 0.10$ kJ/mol and $\Delta s_0 = 0.0002$ kJ/mol were calculated for cyanide. For both phenol and cyanide, the value of $\Delta S_0 < 1$, shows that the process is reversible.

4. Conclusions

The batch studies accompanied in the current study offers important information about biosorption of phenol and cyanide onto saw dust activated carbon (SDAC) in terms of optimum biomass dose, pH, temperature, time and initial concentration for maximum removal of phenol and cyanide

from aqueous solution. The studies designate that SDAC is an effective biosorbent for phenol and cyanide removal. In binary component system the maximum phenol and cyanide biosorption capacity have been established to be 178.85 mg/g and 0.82 mg/g, respectively, with initial concentration of 300 mg/L for phenol and 30 mg/L for cyanide. The Langmuir, Freundlich and Redlich–Peterson adsorption mono component isotherm models were used for a mathematical explanation of the biosorption of phenol and cyanide onto SDAC and it was established that the equilibrium data fitted better to the Redlich–Peterson model in the mono component system. In a binary component system extended Freundlich model indicates a better fit with experimental data. The influence of the existence of phenol and cyanide shows synergism and antagonistic effect, respectively on each other. The biosorption of phenol onto the SDAC follows pseudo second order kinetic and adsorbs through chemisorption while biosorption of cyanide follows second-first order kinetics and adsorbs through physisorption. It is depicted from thermodynamic studies that biosorption of phenol and cyanide onto SDAC was found to be reversible and spontaneous in nature. The biosorption process is found to be endothermic for cyanide and exothermic for phenol. With the benefit of high phenol and cyanide biosorption capacity, the SDAC is to be used as an effective and commercially biosorbent for the removal of phenol and cyanide from aqueous solutions.

Acknowledgements

The authors would like to thank to Ministry of Human Resource Development (MHRD, New Delhi), Government of India for funding this research work. The authors are also grateful to Department of Chemical Engineering and Institute Instrumentation Center of Indian Institute of Technology Roorkee, India for providing facilities and technical support.

References

- Agrawal, B., Balomajumder, C., Thakur, P.K., 2013. Simultaneous co-adsorptive removal of phenol and cyanide from binary solution using granular activated carbon. *Chem. Eng. J.* 228, 655–664.
- Aksu, Z., Acikel, U., 2000. Modelling of a single-staged bioseparation process for simultaneous removal of iron(III) and chromium(VI) by using *Chlorella vulgaris*. *Biochem. Eng. J.* 4, 229–238.
- Aksu, Z., Acikel, U., Kabasakal, E., Tezer, S., 2002. Equilibrium modelling of individual and simultaneous biosorption of chromium (VI) and nickel(II) onto dried activated sludge. *Water Res.* 36, 3063–3073.
- Aksu, Z., Akpınar, D., 2008. Simultaneous adsorption of phenol and chromium (VI) from binary mixtures onto powdered activated carbon. *J. Environ. Sci. Health* 35, 379–405.
- Al-Asheh, S., Banat, F., Al-Omari, R., Duvnjak, Z., 2000. Predictions of binary sorption isotherms for the sorption of heavy metals by pine bark using isotherm data. *Chemosphere* 41, 659–665.
- Allen, S.J., McKay, G., Khader, K.Y.H., 1989. Intraparticle diffusion of basic dye during adsorption on to Sphagnum peat. *Environ. Pollut.* 56, 39–50.
- APHA, 2001. Standards Methods for the Examination of Water and Wastewater, 20th ed. American Public Health Association, Washington, DC.
- ATSDR 2006, Public Health Statement for Cyanide. Agency for Toxic Substances and Disease Registry, Atlanta, GA.
- ATSDR 2008, Toxicological Profile for Phenol. Agency for Toxic Substances and Disease Registry, Atlanta, GA.
- Bandyopadhyay, K., Das, D., Maiti, B.R., 1998. Kinetics of phenol degradation using *Pseudomonas putida* MTCC 1994. *Bioprocess Eng.* 18, 373–377.
- Behnamfard, A., Mohammad, M.S., 2009. Equilibrium and kinetic studies on free cyanide adsorption from aqueous solution by activated carbon. *J. Hazard. Mater.* 170, 127–133.
- Biswas, J., 2013. Evaluation of various method and efficiencies for treatment of effluent from iron and steel industry – a review. *Int. J. Mech. Eng. Rob. Res.* 2, 67–73.
- Busca, G., Berardinelli, S., Resini, C., Arrighi, L., 2008. Technologies for the removal of phenol from fluid streams: a short review of recent development. *J. Hazard. Mater.* 160, 265–288.
- Carvalho, M.F., Duque, A.F., Goncalves, I.C., Castro, P.M.L., 2007. Adsorption of fluorobenzene onto granular activated carbon: isotherm and bioavailability studies. *Bioresour. Technol.* 98, 3424–3430.
- Chung, T.P., Tseng, H.Y., Juang, R.S., 2003. Mass transfer effect and intermediate detection for phenol degradation in immobilized *Pseudomonas putida* systems. *Process Biochem.* 38, 1497–1507.
- Dash, R.R., Balomajumder, C., Kumar, A., 2009. Removal of cyanide from water and wastewater using granular activated carbon. *Chem. Eng. J.* 146, 408–413.
- Desta, M.B., 2013. Batch sorption experiments: Langmuir and Freundlich isotherm studies for the adsorption of textile metal ions onto teff straw (*Eragrostis tef*) agriculture waste. *J. Thermodyn.*, 1–6.
- Dwivedi, C.P., Sahu, J.N., Mohanty, C.R., Mohan, B.R., Meikap, B.C., 2008. Column performance of granular activated carbon packed bed for Pb(II) removal. *J. Hazard. Mater.* 156, 596–603.
- Ekpete, O.A., Horsfall, M., Tarawou, T., 2010. Potential of fluid and commercial activated carbons for phenol removal in aqueous systems. *J. Eng. Appl. Sci.* 5, 39–47.
- Gok, C., Turkozu, D.A., Aytas, S., 2011. Removal of Th(IV) ions from aqueous solution using bi-functionalized algae-yeast biosorbent. *J. Radioanal. Nucl. Chem.* 287, 533–541.
- Gupta, N., Balomajumder, C., Agrawal, V.K., 2012. Adsorption of cyanide on pressmud surface: a modeling approach. *Chem. Eng. J.* 191, 548–556.
- Hameed, B.A., Tan, I.A.W., Ahmad, A.L., 2008. Adsorption isotherm, kinetic modeling and mechanism of 2,4,6-trichlorophenol on coconut husk based activated carbon. *Chem. Eng. J.* 144, 235–244.
- Ho, Y.S., McKay, G., 1998. The kinetics of sorption of basic dyes from aqueous solutions by sphagnum moss peat. *Can. J. Chem. Eng.* 76, 822–826.
- Ho, Y.S., McKay, G., 1998. Sorption of dye from aqueous solution by peat. *Chem. Eng. J.* 70, 115–124.
- Hoa, Y., Ofomaja, A.E., 2006. Pseudo-second-order model for lead ion sorption from aqueous solutions onto palm kernel fiber. *J. Hazard. Mater.* 129, 137–142.
- Huh, J., Song, D., Jeon, Y., 2000. Sorption of phenol and alkylphenols from aqueous solution onto organically modified montmorillonite and applications of dual mode sorption model. *Sep. Sci. Technol.* 35, 243–259.
- Jadhav, D.N., Vanjara, A.K., 2004. Removal of phenol from wastewater using sawdust, polymerized sawdust and sawdust carbon. *Ind. J. Chem. Technol.* 11, 35–41.
- Khalid, N., Rahman, S., Ahmad, S., 2005. Potential of sawdust for the decontamination of lead from aqueous media. *Sep. Sci. Technol.* 40 (12), 2427–2443.
- Kilic, M., Varol, E.A., Putun, A.E., 2011. Adsorptive removal of phenol from aqueous solutions on activated carbon prepared from tobacco residues: equilibrium, kinetics and thermodynamics. *J. Hazard. Mater.* 189 (1–2), 397–403.
- Korhonen, J.T., 2011. Hydrophobic nanocellulose aerogels as floating, sustainable, reusable and recyclable oil adsorbents. *Appl. Mater. Interface* 3, 1813–1816.

- Kowalska, M., Bodzek, M., Bohdziewicz, J., 1998. Biodegradation of phenols and cyanides using membranes with immobilized microorganisms. *Process Biochem.* 33, 189–197.
- Kumar, S., Zafar, M., Prajapati, J.K., Kumar, S., Sivaram Kannepalli, 2011. Modeling studies on simultaneous adsorption of phenol and resorcinol onto granular activated carbon from simulated aqueous solution. *J. Hazard. Mater.* 185, 287–294.
- Lagergren, S., 1898. About the theory of so called adsorption of soluble substances. *K. Sven. Vetensk. Akad. Handl.* 24, 1–39.
- Malik, P.K., 2004. Dye removal from wastewater using activated carbon developed from sawdust: adsorption equilibrium and kinetics. *J. Hazard. Mater.* 113, 81–88.
- Mandi, L., Achak, M., Hafidi, A., Ouazzani, N., 2009. Low cost biosorbent for the removal of phenolic compounds from olive mill wastewater. *OPTIONS Méditerranéennes A* 88, 179–186.
- Mohanty, K., Jha, M., Meikap, B.C., Biswas, M.N., 2005. Removal of chromium (VI) from dilute aqueous solutions by activated carbon developed from *Terminalia arjuna* nuts activated with zinc chloride. *Chem. Eng. Sci.* 60, 3049–3059.
- Moussavi, G., Khosravi, R., 2010. Removal of cyanide from wastewater by adsorption onto pistachio hull wastes: parametric experiments, kinetics and equilibrium analysis. *J. Hazard. Mater.* 183, 724–730.
- Nwugo, B.T., Isaac, N.D., Onche, E.U., 2014. Preparation and characterization of sawdust (cellulose) as an adsorbent for oil pollution remediation. *Int. J. Nat. Sci. Res.* 2, 97–102.
- Panagou, E.Z., Kodogiannis, V.S., 2009. Application of neural networks as a nonlinear modelling technique in food mycology. *Expert Syst. Appl.* 36, 121–131.
- Prasad, A.L., Santhi, T., 2012. Adsorption of hazardous cationic dyes from aqueous solution onto *Acacia nilotica* leaves as an eco friendly adsorbent. *Sustain. Environ. Res.* 22, 113–122.
- Reynel-Avila, H.E., Mendoza-Castillo, D.I., Hernandez-Montoya, V., Bonilla Petriciolet, A., 2011. Multicomponent removal of heavy metals from aqueous solution using low-cost sorbents, in: *Water Production and Wastewaters Treatment*. Edit. Nov. Sci. Pub. 69–99.
- Saltali, K., Sari, A., Aydin, M., 2007. Removal of ammonium ion from aqueous solution by natural Turkish (Yıldızeli) zeolite for environmental quality. *J. Hazard. Mater.* 141 (3), 258–263.
- Santhi, T., Manonmani, S., 2012. Adsorption of Methylene Blue from aqueous solution onto a waste aquacultural shell powders (prawn waste). *Sustain. Environ. Res.* 22, 45–51.
- Saxena, S., Prasad, M., Amritphale, S.S., Chandra, N., 2001. Adsorption of cyanide from aqueous solutions at pyrophyllite surface. *Sep. Purif. Technol.* 24, 263–270.
- Srihari, V., Das, A., 2008. The kinetic and thermodynamic studies of phenol-sorption onto three agro-based carbons. *Desalination* 225, 220–234.
- Srividya, K., Mohanty, K., 2009. Biosorption of hexavalent chromium from aqueous solutions by *Catla catlascales*: equilibrium and kinetics studies. *Chem. Eng. J.* 155, 666–673.
- Subramanyam, B., Das, A., 2009. Study of the adsorption of phenol by two soils based on kinetic and isotherm modeling analyses. *Desalination* 249, 914–921.
- Sulaymon, A.H., Mohammed, A.A., Al-Musawi, T.J., 2013. Competitive biosorption of lead, cadmium, copper, and arsenic ions using algae. *Environ. Sci. Pollut. Res.* 20, 3011–3023.
- Tsibranska, I., Hristova, E., 2011. Comparison of different kinetic models for adsorption of heavy metals onto activated carbon from apricot stones. *Bul. Chem. Commun.* 43, 370–377.
- Uddin, M.T., Islam, M.S., Adedin, M.Z., 2007. Adsorption of phenol from aqueous solution by water hyacinth ash. *J. Eng. Appl. Sci.* 2, 11–17.
- Vedula, R.K., Dalal, S., BaloMajumder, C., 2013. Bioremoval of cyanide and phenol from industrial wastewater: an update. *Biorem. J.* 17, 278–293.
- Viraraghavan, T., Alfaro, F.D.M., 1998. Adsorption of phenol from wastewater by peat, fly ash and bentonite. *J. Hazard. Mater.* 57, 59–70.